Natural Convection in an Externally Heated Enclosure Containing a Local Heat Source

J. L. Zia,* M. D. Xin,* and H. J. Zhang*
Chongqing University, Chongqing, 630030, Sichuan, China

Numerical analysis is carried out for unsteady and steady, two-dimensional, laminar, natural convection heat transfer in an externally heated enclosure containing a local internal heat source. Results are obtained for $Ra_e = 10^3$–10^6, $Ra^* = 3$–3000, $A^* = 0.0333$, $Pr = 0.7$ and $(X_s, Y_s) = (0.5, 0.09091)$. The transient control regime, the equivalent relative intensity of the internal heat source, and the transient equivalent relative intensity of the heat source are defined. Velocity vector plots and temperature profiles in the enclosure are given, and the average and local Nusselt numbers are presented.

Nomenclature

A = area of enclosure
A_s = area of local heat source
A^* = area ratio, A_s/A
H = height of enclosure
k = thermal conductivity
Nu = Nusselt number, Eq. (13)
P = dimensionless pressure $(p + g\rho y)H^2/\rho\alpha^2$
p = pressure
Pr = Prandlt number
q = heat source intensity
Ra_e = external Rayleigh number $g\beta(T_h - T_c)H^3/\nu\alpha$
Ra_i = internal Rayleigh number $g\beta qH^5/\nu\alpha k$
Ra^* = relative intensity of local heat source, Ra_i/Ra_e
Ra^{**} = equivalent relative intensity of heat source, Ra^*A^*
T = temperature
t = time
U = dimensionless velocity in X direction, uH/α
u = velocity in x direction
V = dimensionless velocity in Y direction, vH/α
v = velocity in y direction
X = dimensionless horizontal coordinate, x/H
x,y = coordinate, see Fig. 1
Y = dimensionless vertical coordinate, y/H
α = thermal diffusivity
θ = dimensionless temperature $(T - T_c)/(T_h - T_c)$
β = thermal expansion coefficient
μ = dynamic viscosity
ν = kinematic viscosity
τ = dimensionless time, $\alpha t/H^2$

Subscripts

c = cold surface
tr = transient value
f = fluid
h = hot surface
max = maximum value
s = heat source

Superscript

n = iteration number

Received Jan. 23, 1989; revision received July 10, 1989.

*Professor, Institute of Engineering Thermophysics.

Introduction

In recent years considerable attention has been paid to the study of natural convection in enclosures. A great number of numerical and experimental investigations have been carried out.[1-4]

Natural convection in enclosures induced by internal heat source is widely found in fields of nuclear reactors,[5] geophysics,[6] astrophysics,[7] chemical reactions,[8-9] and others. Natural convection induced by the uniform heat source has been studied widely, e.g., see Refs. 10–20. The numerical and experimental studies of natural convection in enclosures with concentrated heat source have been conducted.[21,22] Yet, most of the studies in the past considered generally the steady natural convection. Unsteady natural convection has not been paid enough attention. What is more, the investigation of natural convection heat transfer in an externally heated enclosure containing a local heat source is sparse. The present paper presents numerical results for the two-dimensional, laminar, natural-convection heat transfer in a square enclosure caused simultaneously by the external heating and a local heat source, which gives rise to unsteady and steady performances.

Governing Equations

The physical situation to be considered is schematically illustrated in Fig. 1. The square enclosure with the two vertical walls at uniform temperatures T_h and T_c and the two horizontal adiabatic walls, contains a local heat source located in the center region of the adiabatic bottom surface. At the initial moment, the enclosure walls and the fluid in it are at the same temperature, and the fluid is motionless. In the range of the present study, the temperature variations are always not large so that the Boussinesq approximation can be accepted. The fluid motion and heat transfer in the enclosure are supposed to be two dimensional. Radiation heat exchange between the walls, viscous dissipation, and compression work are neglected in the energy equation.

For the sake of brevity, the conservation equations of mass, momentum, and energy are directly written in dimensionless form:

$$\frac{\partial U}{\partial X} + \frac{\partial V}{\partial Y} = 0 \tag{1}$$

$$\frac{\partial U}{\partial \tau} + U\frac{\partial U}{\partial X} + V\frac{\partial U}{\partial Y} = -\frac{\partial P}{\partial X} + Pr\left(\frac{\partial^2 U}{\partial X^2} + \frac{\partial^2 U}{\partial Y^2}\right) \tag{2}$$

$$\frac{\partial V}{\partial \tau} + U\frac{\partial V}{\partial X} + V\frac{\partial V}{\partial Y} = -\frac{\partial P}{\partial Y} + Ra_e Pr\theta + Pr\left(\frac{\partial^2 V}{\partial X^2} + \frac{\partial^2 V}{\partial Y^2}\right) \tag{3}$$

$$\frac{\partial\theta}{\partial\tau} + U\frac{\partial\theta}{\partial X} + V\frac{\partial\theta}{\partial Y} = \frac{\partial^2\theta}{\partial X^2} + \frac{\partial^2\theta}{\partial Y^2} + Ra^* \quad (4)$$

where

$$Ra^* = Ra_i/Ra_e = \begin{cases} C & X\epsilon[X', X''],\ Y\epsilon[Y', Y''] \\ 0 & \text{other} \end{cases} \quad (5)$$

Ra^* is the ratio of the internal Rayleigh number Ra_i to the external Rayleigh number, Ra_e. It reflects the relative intensity of the local heat source.

The temperature and velocity boundary conditions at the walls of the enclosure and the initial condition are

$$U = 0,\ V = 0,\ \frac{\partial\theta}{\partial Y} = 0 \qquad Y = 0,1,\ \tau > 0 \quad (6)$$

$$U = 0,\ V = 0,\ \theta = 1 \qquad X = 0,\ \tau > 0 \quad (7)$$

$$U = 0,\ V = 0,\ \theta = 0 \qquad X = 1,\ \tau > 0 \quad (8)$$

$$U = 0,\ V = 0,\ \theta = 0,\ Ra^* = 0 \qquad \tau = 0 \quad (9)$$

In the present study, the governing equations are numerically solved by the control-volume-based, finite-difference method. The grid layout is such that the solid-fluid interface forms a control volume face for the neighboring grid points. The grid was packed close to the walls and the local internal heat source, and the nonuniformity of the grid changes with Ra^* and Ra_e. The forward difference is employed for the partial time derivative, the central differencing scheme for the diffusivity terms, and the upwind difference type scheme for the convective terms. The alternating direction implicit (ADI) method is used to solve the system of transient elliptic equations. Because of the nonlinearity of the momentum equations, the coupling of fluid motion and heat transfer, and the velocity-pressure coupling, the semi-implicit method for pressure-linked equation (SIMPLE) algorithm[23] is utilized, but the pressure correction iteration proceeds until the sum of residual mass of all grids is less than a small number. The time step is made 0.0001–0.0005.

A 24×24 grid is finally chosen after a number of trial numerical experiments. For example, a comparison of the results from a 24×24 grid with the corresponding results for a 43×43 grid at $Ra_e = 10^5$, and $Ra^* = 1500$ shows a deviation of 0.373% for θ_{max}, of 2.64% for V_{max}, and of 1.07% for the average Nusselt number. Also the velocity and temperature profiles obtained with the two grids are almost identical to each other, and the local Nusselt numbers along the hot and cold surfaces obtained by the two grids are very close to each other. Again, the 24×24 grid solutions agree well with the 43×43 grid results for $Ra_e = 10^6$ and $Ra^* = 1500$.

When the following condition is satisfied, the steady state of the flow and heat transfer in the enclosure are considered to be reached:

$$\left|\frac{Nu^{n+1} - Nu^n}{Nu^{n+1}}\right| < 5*10^{-6} \quad (10)$$

The overall energy balance should be satisfied in the steady state, and this requires:

$$R = -\int_0^1 \frac{\partial\theta}{\partial X}\bigg|_{X=0} dY + Ra^{**} + \int_0^1 \frac{\partial\theta}{\partial X}\bigg|_{X=1} dY = 0 \quad (11)$$

$$Ra^{**} = A^* Ra^* \quad (12)$$

where Ra^{**} is called the equivalent relative intensity of the internal heat source or the equivalent Rayleigh number ratio, which can reflect more reasonably the influence of the local internal heat source with different areas. The A^* denotes the partition of the area occupied by the local heat source or the area ratio. The numerical results show that in all cases considered here, R differs from zero only in the fifth significant digit after the decimal point.

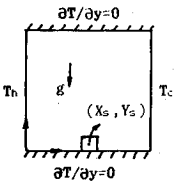

Fig. 1 Scheme of the enclosure containing a local heat source.

The present results are compared with those of Refs. 24–26 for natural convection in an externally heated enclosure ($Ra^* = 0$) as illustrated in Table 1. As may be observed from this table, good agreement with the bench-mark solution is obtained—especially for the lower Rayleigh numbers. At higher external Rayleigh numbers, the present solution provides a higher Nusselt number than that of Refs. 24–25 but lower than that of Ref. 26.

It can be seen from Eqs. (1-4) and (11) that for natural convection in the externally heated square enclosure containing a local heat source, the main controlling parameters are Pr, Ra_e, A^*, Ra^*, or Ra^{**} and the location of the local heat source (X_s, Y_s). Thus,

$$Nu = -\int_0^1 \frac{\partial\theta}{\partial X} dY = f\,(Pr,\ Ra_e,\ A^*,\ Ra^{**},\ X_s, Y_s) \quad (13)$$

It should be pointed out that in Eq. (4) or (11), Ra^* or Ra^{**} could be used as the independent parameter instead of Ra_i.

Results and Discussion

Velocity Vectors and Isotherms

Several typical velocity vector plots and isotherms are shown in Figs. 2. It can be observed that five different flow patterns occur in the externally heated square enclosure containing a local heat source with the change of Ra^{**} under the condition of given A^* and Ra_e. For $Ra^{**} \ll 1.0$, the flow and heat transfer in the externally heated enclosure with a local heat source are almost the same as those of the only externally heated one, and a single clockwise flow is formed. For $Ra^{**} \sim 1$, the fluid in the enclosure still flows clockwise, but the temperature profile changes as shown in Fig. 2a. This kind of flow mode is defined as the first flow pattern. However, as Ra^{**} increases, two rolls are present as shown in Fig. 2b. The larger roll is a clockwise flow moving downwards along the cold surface and upwards along the hot surface. The other weak eddy is formed in the bottom corner of the hot surface side with a counterclockwise flow direction. Furthermore, the intensity of the weak eddy is much lower than that for the large roll. This kind of flow mode is defined as the second flow pattern. It should be pointed out here (but not shown in this paper) that when A^* increases or when the location of the local heat source deviates to some extent from the bottom adiabatic surface, in the second pattern, the weak counterclockwise eddy takes place in the top corner of the hot surface side. When Ra^{**} goes up further, the flow in the enclosure enters into the third flow pattern as seen in Fig. 2c. That is, two weak counterclockwise eddies occur in the top and bottom corner of the hot surface side, respectively, and a large clockwise roll is formed in the other region of the enclosure. With Ra^{**} continuing to increase, a counterclockwise roll appears along the overall hot surface, and a larger clockwise roll appears in the other region of the enclosure. But the intensity of the counterclockwise roll is still much smaller than that of the clockwise roll as shown in Fig. 2d. This kind of flow mode is defined as the fourth flow pattern. When Ra^{**} becomes larger, the intensity of the counterclockwise roll increases, and

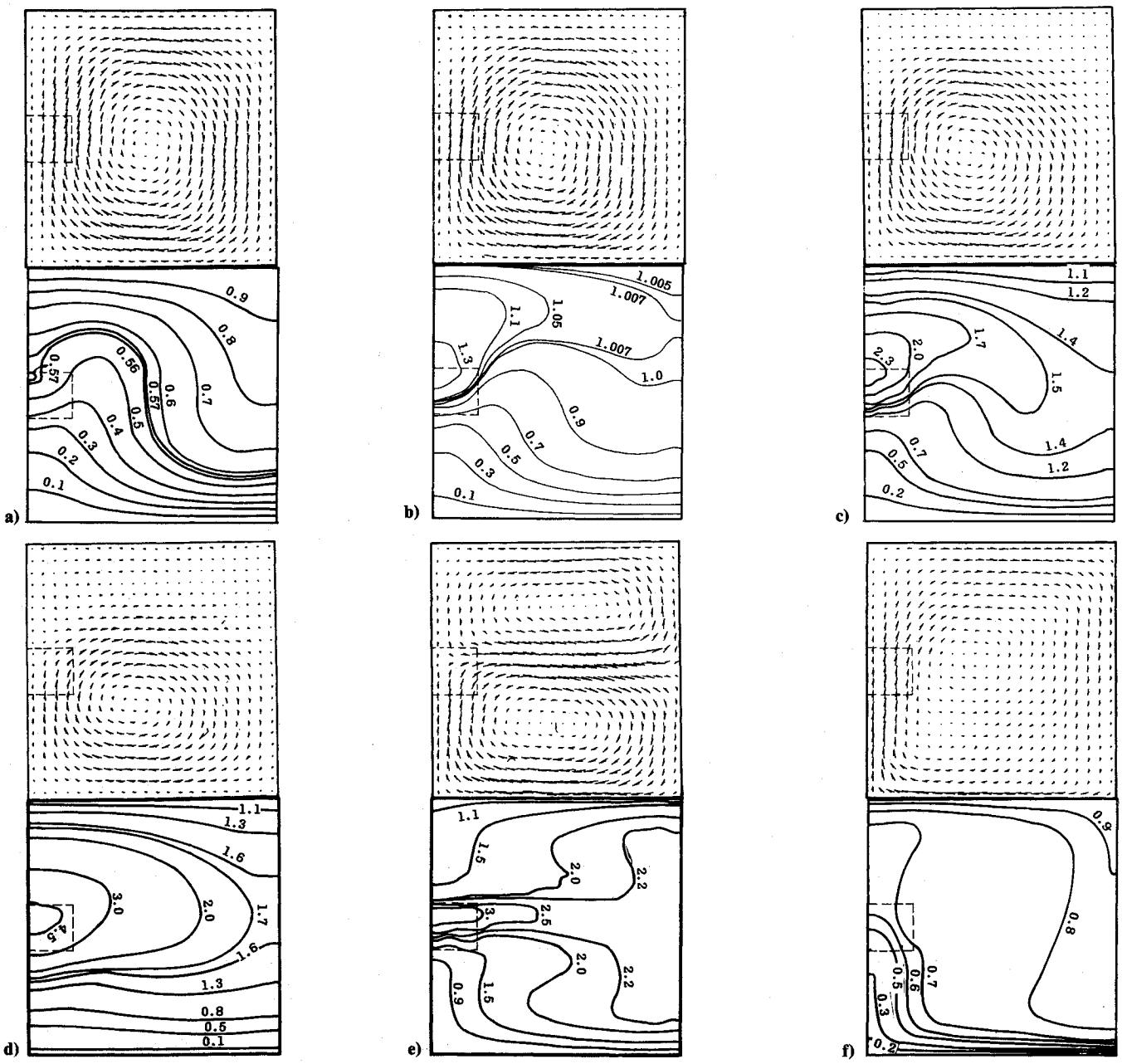

Fig. 2 Velocity vector plots and isotherms: a) $Ra_e = 10^4$, $Ra^{**} = 0.9917$, $V_{max} = 21.4$; b) $Ra_e = 10^4$, $Ra^{**} = 4.56$, $V_{max} = 28.9$; c) $Ra_e = 10^4$, $Ra^{**} = 9.917$, $V_{max} = 36.93$; d) $Ra_e = 10^3$, $Ra^{**} = 9.917$, $V_{max} = 10.4$; e) $Ra_e = 10^5$, $Ra^{**} = 39.67$, $V_{max} = 277.8$; f) $Ra_e = 10^6$, $Ra^{**} = 9.917$, $V_{max} = 317.61$.

Table 1 Comparison of solutions for natural convection in an enclosure

Ra_e	10^3				10^4				10^5				10^6			
	1	2	3	4	1	2	3	4	1	2	3	4	1	2	3	4
Nu	1.108	1.118	1.141	1.139	2.201	2.243	2.29	2.31	4.430	4.519	4.964	4.894	8.754	8.799	10.39	10.28
Nu_{max}	1.496	1.505	1.540	1.533	3.482	3.528	3.840	3.76	7.626	7.717	8.930	8.840	17.87	17.93	21.41	21.30
Nu_{min}	0.720	0.692	0.727	0.720	0.643	0.586	0.670	0.65	0.824	0.729	1.010	0.928	1.232	0.989	1.58	1.56

1—Markatos-Perikleous[25] 2—de Vahl Davis[24] 3—Hadjisophocleous-Sousa-Venart[26] 4—present solution

the area occupied by it also tends to be larger. When Ra^{**} is large enough, which means that the magnitude of Ra_i considerably exceeds that of Ra_e, the flowfield consists of the two counter-rotating convective rolls, which have nearly identical intensities. The interface of the two rolls is located in the vertical central plane of the local heat source with a little deviation towards the hot surface. This kind of flow mode is defined as the fifth flow pattern.

It is interesting to define a transient equivalent Rayleigh number ratio, Ra^{**}_{tr}, which is the Ra^{**} corresponding to the transition from the first flow pattern to the second one. Ra^{**}_{tr} increases with an increase in the external Rayleigh number Ra_e. For example, $Ra^{**}_{tr} \doteq 1.785$ at $Ra_e = 10^3$, $Ra^{**}_{tr} \doteq 14.7$ at $Ra_e = 10^6$. The dependence of Ra^{**}_{tr} on Ra_e is shown in Fig. 3 and can be correlated by the following equation:

$$Ra^{**}_{tr} = 0.212 Ra_e^{0.307} \tag{14}$$

The maximum standard deviation between Eq. (14) and the numerical results is 1.625%.

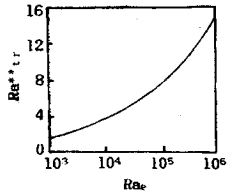

Fig. 3 Change of Ra^{**}_{tr} with Ra_e.

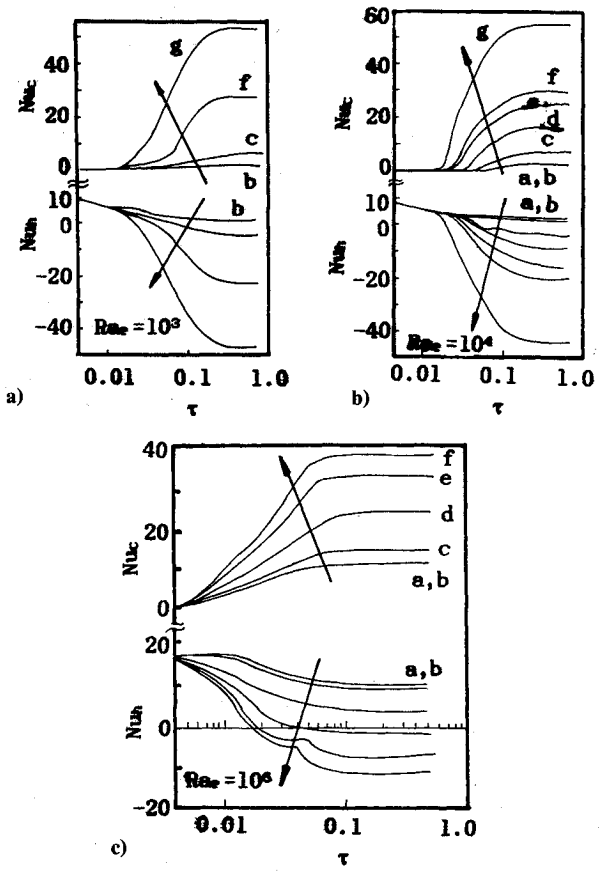

Fig. 4 Time history of the average Nu for the hot and cold surfaces, Ra^{**} = a) 0.09917; b) 0.9917; c) 9.917; d) 24.79; e) 39.67; f) 49.59; g) 99.17.

In the first flow pattern ($Ra^{**} < Ra^{**}_{tr}$), the external heating controls the flow and heat transfer in the enclosure, and the effect of the local heat source is small and negligible, especially for $Ra^{**} < 0.1$. In the fifth flow pattern, the local heat source controls the flow and heat transfer in the enclosure. In the situation of the second, third, and fourth flow patterns, the effects of both the external heating and the local heat source on the flow and heat transfer are not negligible. We define these three flow patterns as the transient control regime. Thus with the change of Ra^{**} at a given Ra_e or Ra_e at a given Ra^{**}, the flow in the externally heated square enclosure containing a local heat source can also be divided into three flow regimes: the external heating control regime, the transient control regime, and the internal heat source control regime. It is found through the numerical investigation that the transient control regime occurs in the range of $1.785 < Ra^{**} < 48.5$ for $10^3 < Ra_e < 10^6$.

Because the influence of the external heating on the fluid flow near the hot surface is opposite to that of the local heat source and one side of the local heat source coincides with the bottom surface, and because of the walls of the bottom-left corner of the enclosure, a counterclockwise eddy is first formed at the bottom-left corner in the second flow pattern. At that time, the local heat source still has a much smaller

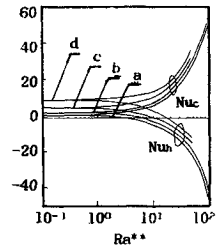

Fig. 5 Effect of Ra^{**} on the average Nu, Ra_e = a) 10^3; b) 10^4; c) 10^5; d) 10^6.

effect on the flow and heat transfer in the enclosure than the external heating. In the fourth flow pattern, the influence of the former becomes larger than that of the latter, and the fluid moves downwards along the hot surface. It should be mentioned that the convective flow near the hot surface is quite weak compared to that on the side of the cold surface, and the fluid near the hot surface is nearly stagnant when the flow just enters into the fourth flow pattern.

As shown in Figs. 2, the characteristics of the flow and heat transfer in the externally heated enclosure with a local heat source differs for the different Ra_e at the condition of given Ra^{**}. Natural convection becomes more intensive with an increase in Ra_e. Moreover, the range of Ra^{**} corresponding to the transient control regime changes towards larger value as Ra_e increases. For instance, at $Ra^{**} = 9.917$, the flow in the enclosure is in the four-flow pattern for $Ra_e = 10^4$, and in the first flow pattern for $Ra_e = 10^6$.

Change of the Average Nusselt Number with Time

The variations of the average Nusselt number of both the hot and cold surfaces with dimensionless time at various Ra_e and Ra^{**} are shown in Fig. 4. As observed in this figure, the time required to reach the steady state τ_s decreases with increasing Ra_e. For example, $\tau_s \doteq 0.94$ at $Ra_e = 10^3$, and $\tau_s \doteq 0.51$ at $Ra_e = 10^6$. For the cold surface, Nu_c always becomes larger with rising τ, but the increasing speed with time varies with Ra_e and Ra^{**}. For the hot surface, when the flow and heat transfer in the enclosure are controlled by the external heating, Nu_h decreases with increasing τ but always is positive. This implies that the hot surface is significant in heating the fluid in the enclosure. However, as Ra^{**} increases, which means the increasing influence of local heat source, Nu_h descends to zero and then becomes negative. The negative Nu_h indicates that the fluid in the enclosure is cooled by the hot surface. The dimensionless time corresponding to the zero average Nusselt number decreases with an increase in Ra^{**} for the constant Ra_e.

Average Nusselt Number

Figure 5 shows the influence of Ra^{**} on Nu_h and Nu_c at various Ra_e values. In the external heating control regime, the effect of Ra^{**} on Nu_c is small—especially for $Ra^{**} < 0.1$, and the influence of the heat source is negligible. The same is true for the hot surface. In the transient control regime and the internal heat source control regime, a drastically different situation occurs. For the cold surface, Nu_c always increases monotoneously with Ra^{**}. For the hot surface, in the heat source control regime, the hot surface plays a role in cooling the fluid in the enclosure (Nu_h is negative) and $|Nu_h|$ increases with Ra^{**}; in the transient control regime, the change of Nu_h with Ra^{**} undergoes a process from positive to negative. In other words, when the effect of external heating is larger than that of the local heat source, the hot surface plays a role in heating the fluid in the enclosure, and when the former is less than the latter, the hot surface cools the fluid in the enclosure. At some Ra^{**} value, $Nu_h = 0$, which explains the zero average heat flow through the hot surface, but of course it does not mean that the local Nu_h is consistently equal

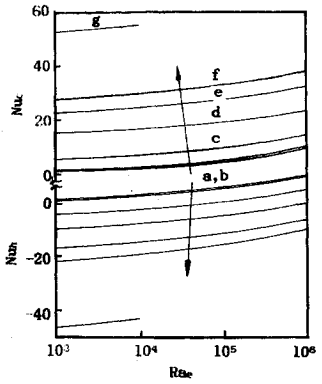

Fig. 6 Variation of the average Nu with Ra_e, Ra^{**} = a) 0.09917; b) 0.9917; c) 9.917; d) 24.79; e) 39.67; f) 49.59; g) 99.17.

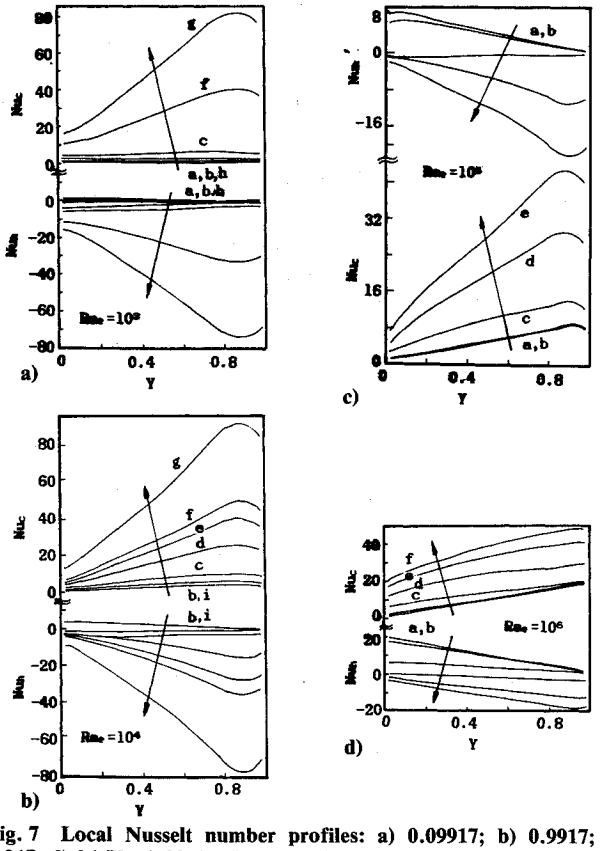

Fig. 7 Local Nusselt number profiles: a) 0.09917; b) 0.9917; c) 9.917; d) 24.79; e) 39.67; f) 49.59; g) 99.17 h) 3.63; i) 4.958.

to zero. Furthermore, Ra^{**} corresponding to $Nu_h = 0$ increases with Ra_e. As shown in Fig. 6, Nu_c increases with Ra_e, and the change of Nu_h with Ra_e is complicated due to the effect of Ra^{**}. The internal heat source plays a role in decreasing the heat transfer of the hot surface towards the enclosure and in enhancing heat transfer of the cold surface.

The average Nusselt number in the steady state can be given by Eq. (15)

$$Nu_c = 0.368 Ra_e^{0.122} Ra^{**0.812}$$

$$10^3 < Ra_e < 10^6, \qquad 4.9 < Ra^{**} < 14.88 \tag{15a}$$

$$Nu_c = 0.711 Ra_e^{0.0565} Ra^{**0.83}$$

$$10^3 < Ra_e < 10^6, \qquad 14.9 < Ra^{**} < 99.17 \tag{15b}$$

$$Nu_h = Nu_c - Ra^{**} \tag{15c}$$

The maximum standard deviation from Eq. (15) is 6.22%.

Local Nusselt Number

Figure 7 shows the variation of the local Nu_h and Nu_c with Ra_e and Ra^{**}. In all cases considered, there exists a maximum local Nusselt number. As far as the cold surface is concerned, the maximum local Nu_c always occurs at the top-right corner of the enclosure, and its location goes slightly downwards with increasing Ra_e for a given Ra^{**} or Ra^{**} for a given Ra_e. In the transient control regime, there occur a maximum local Nu_c at the top-right corner and a minimum one at the bottom-right corner of the enclosure. As far as the hot surface is concerned, the situation is much more complicated. In the external heating control regime, the maximum local Nu_h occurs at the bottom-left corner of the enclosure, a position in the vicinity of the region where the fluid from the opposite surface encounters the surface. As Ra^{**} increases, the location of the maximum local Nu_h moves upwards along the hot surface. In the heat source control regime, the maximum local $|Nu_h|$ occurs in the vicinity of the top-left corner of the enclosure. In the transient control regime, the maximum local Nu_h can be positive or negative, that is, some part of the hot surface plays a role in heating the fluid in the enclosure and the other in cooling the fluid. In other words, the local Nusselt number attains its maximum value in the vicinity of the region where the fluid from the interior or the opposite surface encounters the surface.

Conclusions

1) The external Rayleigh number Ra_e and the relative intensity of internal heat source Ra^* or the equivalent relative intensity of the internal heat source Ra^{**} have a drastic influence on natural convection heat transfer in an enclosure. For constant Ra_e (or Ra^{**}), there exist five flow patterns in the enclosure with increasing Ra^{**} (or Ra_e). The second, third, and fourth flow patterns are also defined as the transient control regime. Under the condition of $Ra_e = 10^3 \sim 10^6$, the range of Ra^{**} corresponding to the transient control regime is approximately given by $1.785 < Ra^{**} < 48.5$.

2) The Ra^{**} corresponding to the transient from the first flow pattern to the second flow pattern increases with an increase in Ra_e, and the range of Ra^{**} corresponding to the transient control regime becomes larger.

3) For constant Ra_e, Nu_c increases with Ra^{**}, and the change of Nu_h with Ra^{**} is relatively complicated. The internal heat source plays a role in decreasing the heat transfer of the hot surface towards the enclosure and in enhancing the heat transfer at the cold surface.

4) The maximum local Nu_c occurs near the top of the cold surface, and its position moves slightly downwards with increasing Ra_e. The location of the maximum local Nu_h moves from the bottom to the top of the hot surface when Ra^{**} increases.

5) The unsteady characteristics of natural convection in the externally heated enclosure containing a local heat source are different for different Ra_e or Ra^{**}. When Ra^{**} or Ra_e increases, the dimensionless time corresponding to $Nu_h = 0$ decreases, and the time required to reach the steady state decreases. Moreover, Ra^{**} corresponding to $Nu_h = 0$ increases with increasing Ra_e.

References

[1]Ostrach, S., "Natural Convection in Enclosures," *Advances in Heat Transfer*, Vol. 8, 1972, p. 161.

[2]Catton, I., "Natural Convection in Enclosures," *Proceedings of the 6th International Heat Transfer Conference*, Vol. 1, Hemisphere, Washington, DC, 1987, p. 13.

[3]Ostrach, S., "Natural Convection Heat Transfer in Cavities and Cells," *Proceedings of the 7th International Heat Transfer Conference*, Vol. 1, Hemisphere, Washington, DC, 1982, p. 365.

[4]Hoogendoorn, C. J., "Natural Convection in Enclosures," *Proceedings of the 8th International Heat Transfer Conference*, Vol. 1, Hemisphere, Washington, DC, 1986, p. 111.

[5]Bajorek, S. M. and Lloyd, R. J., "Experimental Investigation of Natural Convection in Partitional Enclosures," *Journal of Heat Transfer,* Vol. 104, No. 3, 1982, p. 527.

[6]Chang, L. C., Lloyd, R. J., and Yang, K. T., "A Finite Difference Study of Natural Convection in Complex Enclosures," *Proceedings of the 7th International Heat Transfer Conference,* Vol. 2, Hemisphere, New York, 1982, p. 183.

[7]Chang, L. C., Yang, K. T., and Lloyd, R. J., "Radiation-Convection Interaction in Two-Dimensional Complex Enclosures," *Journal of Heat Transfer,* Vol. 105, No. 1, 1983, p. 89.

[8]Kim, D. M. and Viskanta, R., "Study of the Effects of Wall Conductance on Natural Convection in Differently Oriented Square Cavities," *Journal of Fluid Mechanics,* Vol. 44, 1984, p. 153.

[9]Sernas, V. and Lee, E. I., "Heat Transfer in Air Enclosures of Aspect Ratio Less Than One," American Society of Mechanical Engineers, New York, ASME Paper 78-WA/HT-7, Dec. 1978.

[10]Baker, L., Faw, R. E., and Kulacki, A. F., "Postaccident Heat Removal—Part I, Heat Transfer Within an Internally Heated, Nonboiling Liquid Layer," *Nuclear Science and Engineering,* Vol. 61, No. 2, 1976, p. 222.

[11]Mckenzie, D. P., Roberts, J. M., and Meiss, O. N., "Convection in the Earth's Mantle: Towards a Numerical Simulation," *Journal of Fluid Mechanics,* Vol. 62, 1974, p. 465.

[12]Farouk, B., "Turbulent Thermal Convection in an Enclosure with Internal Heat Generation," *Journal of Heat Transfer,* Vol. 110, No. 1, 1988, p. 126.

[13]Lee, R. J., Landram, C. S., and Miles, J. C., "Natural Convection of a Heat Generating Fluid Within Closed Vertical Cylinders and Spheres," *Journal of Heat Transfer,* Vol. 58, No. 1, 1976, p. 55.

[14]Bergholz, R. F., "Natural Convection of a Heat Generating Fluid in a Closed Cavity," *Journal of Heat Transfer,* Vol. 102, No. 2, 1980, p. 242.

[15]Desoclo, L. M., Misici, L., and Polzonetti, A., "Natural Convection in Heat Generating Fluid in Cavities," American Society of Mechanical Engineers, New York, ASME Paper 79-WT/HT-95, 1979.

[16]Greene, G. A., Irvine, T. F., and Jones, O. C., Jr., "Experimental and Analytical Study of Natural Convection Heat Transfer of Internally Heated Fluids," *Proceedings of the 7th International Heat Transfer Conference,* Vol. 2, Hemisphere, Washington, DC, 1982, p. 135.

[17]Barakat, H. A., "Transient Laminar Free Convection Heat and Mass Transfer in Two-Dimensional Closed Containers Containing Distributed Heat Sources," American Society of Mechanical Engineers, ASME Paper 65-WA/HT-28, 1965.

[18]Essam, P., "Free Convection of Heat Generating Fluid in Cylindrical Tanks," *Nuclear Engineering and Design,* Vol. 11, No. 1, 1969, p. 57.

[19]Acharya, S. and Goldstein, R. J., "Natural Convection in an Externally Heated Vertical or Inclined Square Box Containing Internal Energy Sources," *Journal of Heat Transfer,* Vol. 107, No. 4, 1985, p. 855.

[20]Lee, J. H. and Goldstein, R. J., "An Experimental Study on Natural Convection Heat Transfer in an Inclined Square Enclosure Containing Internal Energy Sources," *Journal of Heat Transfer,* Vol. 110, No. 2, 1988, p. 345.

[21]Turner, B. L. and Flack, R. D., "The Experimental Measurement of Natural Convection Heat Transfer in Rectangular Enclosure with Concentrated Energy Sources," *Journal of Heat Transfer,* Vol. 102, No. 2, 1980, p. 236.

[22]Chu, H. H. and Churchill, S. W., "The Effect of Heater Size, Location, Aspect Ratio, and Boundary Conditions on Two-Dimensional, Laminar, Natural Convection in Rectangular Channels," *Journal of Heat Transfer,* Vol. 98, No. 2, 1976, p. 194.

[23]Patanka, S. V., *Numerical Heat Transfer and Fluid Flow,* McGraw-Hill, New York, 1980, p. 126.

[24]de Vahl Davis, G., "Natural Convection of Air in a Square Cavity—A Bench Mark Solution," *International Journal of Numerical Methods in Fluids,* Vol. 3, 1983, p. 249.

[25]Markatos, N. C. and Perikleous, K. A., "Laminar and Turbulent Natural Convection in an Enclosured Cavity," *International Journal of Heat and Mass Transfer,* Vol. 27, No. 5, 1984, p. 755.

[26]Hadjisophocleous, G. V., Sousa, A. C. M., and Venart, J. E. S., "Prediction of Transient Natural Convection in Enclosures of Arbitrary Geometry Using a Nonorthogonal Numerical Model," *Numerical Heat Transfer,* Vol. 13, No. 3, 1988, p. 373.